*Semiconductor Physics, Quantum Electronics & Optoelectronics, 2024. V. 27, No 2. P. 151-156.*

*Semiconductor physics*

# Electronic and magnetic properties of $Zn_{1-x}Mn_xSe:Fe^{2+},Cr^{2+}$ (x = 0.3) single crystals

**D.V. Savchenko[1,2,*], I.V. Ivanchenko[3], N.A. Popenko[3], B.E. Bekirov[3], E.N. Kalabukhova[4]**

[1]*National Technical University of Ukraine "Igor Sikorsky Kyiv Polytechnic Institute" 37, Beresteiskyi Avenue, 03056 Kyiv, Ukraine*
[2]*Technical Center NAS of Ukraine, 13, Pokrovs'ka str., 04070 Kyiv, Ukraine*
[3]*O. Usikov Institute for Radiophysics and Electronics, NAS of Ukraine, 12, Proskura str., 61085 Kharkiv, Ukraine*
[4]*V. Lashkaryov Institute of Semiconductor Physics, NAS of Ukraine, 41, prospect Nauky, 03028 Kyiv, Ukraine*
[*]*Corresponding author e-mail: dariyasavchenko@gmail.com*

**Abstract.** We report the first study of $Zn_{1-x}Mn_xSe:Fe^{2+},Cr^{2+}$ ($x = 0.3$) crystals by continuous wave (CW) and pulsed electron paramagnetic resonance (EPR) spectroscopic techniques. Using the advantages of pulsed EPR, spin Hamiltonian parameters for $Mn^{2+}$ ions were obtained ($g_{\|} = g_{\perp} = 2.0060(3)$, $A_{\|} = A_{\perp} = 61.84 \cdot 10^{-4}$ cm$^{-1}$, and $D = -7.1 \cdot 10^{-4}$ cm$^{-1}$). The temperature dependence of the spin relaxation times of $Mn^{2+}$ ions was described using the Orbach process for $T_M^{-1}$ and the Raman mechanisms for $T_1^{-1}$. The spin Hamiltonian parameters for $Cr^{2+}$ ions were determined from the analysis of the angular dependence of CW EPR spectra ($g_{\perp} = 1.98$, $g_{\|} = 1.961$, $D = -2.48$ cm$^{-1}$, and $a = 0.02$ cm$^{-1}$). Moreover, an anisotropic ferromagnetic resonance (FMR) line was observed, the nature of which has yet to be clarified.

**Keywords:** EPR, transition metals, zinc selenide.

https://doi.org/10.15407/spqeo27.02.151
PACS 61.72.uj, 71.20.Be, 76.30.-v

Manuscript received 13.03.24; revised version received 15.05.24; accepted for publication 19.06.24; published online 21.06.24.

## 1. Introduction

Zinc selenide (ZnSe) materials belong to the II-VI group semiconductor compounds. They have a wide bandgap (~ 2.7 eV at 300 K), high refractive index, transparency, optical nonlinearity, electrical conductivity, and electron mobility. The unique combination of optical, electronic, and structural properties enables the utilization of ZnSe for a wide range of applications spanning from infrared optics and laser technology to semiconductor devices and medical imaging.

In particular, an actual task for researchers is the elaboration of high-power laser materials based on high optical-quality crystalline ZnSe, operating in the mid-infrared spectral range of 4 to 6 μm with potential applications for infrared countermeasures, air pollutants measurements, biomedical diagnostics, free-space communications, target illumination, range-finding, *etc*. It is well known that when ZnSe (having unfilled d-shells) is doped with transition metal ions, 3*d* and 4*p* orbitals can be mixed at non-centrosymmetric lattice sites [1], inducing transitions between the *d* levels. As a result, mid-wave infrared radiation is obtained owing to these new electronic transitions [2].

Recently, compact iron (Fe)-doped ZnSe-based solid-state lasers have been widely studied. A $Fe^{2+}$-doped active material can be pumped by sources generating radiation with the wavelengths near 3 μm (*e.g.*, chromium (Cr)-doped ZnSe solid-state active materials), which would match the $Fe^{2+}$ ion absorption maximum [3]. Another way to pump $Fe^{2+}$ ions is to utilize the energy transfer from $Cr^{2+}$ to $Fe^{2+}$ ions in co-doped ZnSe materials. According to [4], a fluorescence spectrum of $Cr^{2+}$ ions (donors) should overlap with the absorption spectrum of $Fe^{2+}$ ions (acceptors) to obtain the energy transfer in ZnSe.

It was reported in [5] that absorption and fluorescence spectra of $Cr^{2+}$ ions in $Zn_{1-x}Mn_xSe$ solid solutions are shifted toward longer wavelengths as compared to the spectra of $Cr^{2+}$ in ZnSe crystals. Since the shape of the short-wavelength part of an absorption spectrum of $Fe^{2+}$ ions remains almost unchanged, there is a stable shift of the long-wavelength part containing the absorption maximum toward longer wavelengths with the increase of the content (x) of manganese (Mn) ions in the ZnSe matrix.

Recently, a $Cr^{2+} \rightarrow Fe^{2+}$ energy transfer process in $Zn_{1-x}Mn_xSe:Fe^{2+},Cr^{2+}$ ($x = 0.3$) crystals along with gain-

switched laser operation under excitation with short-pulse (200 ns) radiation with the wavelength of 1735 nm was reported [6]. The laser operation under long-pulse (1 ms, 10 Hz, and λ = 1940 nm) pumping by thulium-doped fiber laser was shown [7].

Electron paramagnetic resonance (EPR) is a powerful spectroscopic technique used to study electronic and magnetic properties of materials with unpaired electrons, such as ZnSe co-doped with transition metal ions. ZnSe:Mn and ZnSe:Cr materials are widely studied by the EPR technique [see *e.g.*, 8, 9]. In [10, 11], the results of EPR study of $Cr^{2+}$, $Co^{2+}$, $Fe^{2+}$, and $Er^{3+}$ dopant ions in ZnSe were reported. The EPR measurements on ZnSe co-doped with $Fe^{3+}$ and $Cr^{1+}$ ions were performed in [12]. $Fe^{3+}$, $Mn^{2+}$, $Fe^{2+}$, and $Cr^{2+}$ centers and monoclinic $Fe^{3+}$ complexes locally compensated by $Cu^{+}$ ions in ZnSe:Fe crystals were also revealed by the EPR method [13]. However, no EPR data was reported for $Zn_{1-x}Mn_xSe:Fe^{2+},Cr^{2+}$ crystalline materials.

This paper presents a comprehensive study of $Zn_{1-x}Mn_xSe:Fe^{2+},Cr^{2+}$ crystals by continuous wave (CW) and pulsed EPR methods. The electronic and magnetic properties of the samples under study are obtained.

## 2. Materials and methods

$Zn_{1-x}Mn_xSe:Fe^{2+},Cr^{2+}$ ($x$ = 0.3) crystalline samples were synthesized by the high-pressure Bridgman method. The samples were doped with $Cr^{2+}$ and $Fe^{2+}$ active ions during the synthesis process according to the procedure described in [14]. The $Cr^{2+}$ and $Fe^{2+}$ concentrations were about $3\cdot10^{18}$ and $5\cdot10^{18}$ $cm^{-3}$, respectively. The polished samples thickness was 2.6 mm. The samples were cut in (110) plane, where the [001] direction is in the plane.

Continuous wave and pulsed EPR measurements were performed in the X-band frequency range (~9.4 GHz) using a Bruker ELEXSYS EPR E580 spectrometer equipped with an ER 4112HV variable temperature helium-flow cryostat. Low-temperature EPR measurements in CW and pulsed mode were performed on the SAFMAT research infrastructure (Institute of Physics of the Czech Academy of Sciences, Prague, Czech Republic).

CW EPR measurements were performed using a ER 4122 SHQE SuperX High-Q cavity at the following parameters: microwave power of 0.4743 mW, modulation frequency of 100 kHz, modulation amplitude of 0.4 mT, conversion time of 60 ms, and spectral resolution of 4096 points. A standard DPPH free radical with $g$ = 2.0036 was used as a reference sample.

Electron spin echo (ESE) signal decay traces were recorded using a primary echo sequence, π/2 − τ − π − τ − echo, by increasing the interpulse delay τ of the primary echo sequence with the pulse lengths: π/2 = 16 ns, τ = 400 ns, π = 32 ns with the short repetition time of 4 μs. ESE inversion-recovery experiment was performed using a three-pulse sequence: π − $T$ − π/2 − τ − π − τ −echo with π = 30 ns, $T$ = 400 ns, π/2 = 16 ns, τ = 400 ns, and π = 32 ns.

Field-sweep (FS) ESE spectra were recorded using a two-pulse Hahn echo sequence π/2 − τ − π − τ − echo with the pulse lengths π/2 = 16 ns, τ = 400 ns, and π = 32 ns.

The CW EPR and FS ESE spectra were simulated by the EasySpin 5.2.28 software package [15] using the 'pepper' function and 'matrix' diagonalization method.

For simulation of the EPR spectra of $Mn^{2+}$ ($S$ = 5/2, $I$ = 5/2) and $Cr^{2+}$ ($S$ = 2, $I$ = 3/2) ions, the following spin Hamiltonian was used:

$$H_0 = g_{\parallel}\mu_B B_z S_z + g_{\perp}\mu_B\left(B_x S_x + B_y S_y\right) + D\left[S_z^2 - \frac{1}{3}S(S+1)\right] + \\ + \frac{a}{6}\left[S_x^4 + S_y^4 + S_z^4 - \frac{1}{5}(S+1)\left(3S^2+3S-1\right)\right] + \\ + \frac{F}{180}\left[\begin{matrix}35S_z^4 - 30S(S+1)S_z^2 + 25S_z^2 - 6S(S+1) + \\ + 3S^2(S+1)^2\end{matrix}\right] + \\ + A_{\parallel}S_z I_z + A_{\perp}\left(S_x I_x + S_y I_y\right) + Q\left[I_z^2 - \frac{1}{3}I(I+1)\right] - g_N\mu_N \vec{B}\cdot\vec{I}, \quad (1)$$

where $g_{\parallel}$ and $g_{\perp}$ are the $\vec{g}$ -tensor components of spectroscopic splitting, $g_N$ is the nuclear $g$-factor, $\mu_B$ is the Bohr magneton, $\mu_N$ is the nuclear magneton, $\vec{B}$ is the applied magnetic field, $D = 3B_2^0$ is the second-order spin operator, representing a component of the crystalline electric field that is axially symmetric with respect to the $\vec{c}$ -axis, $a = 24B_4^4$ is the fourth-order spin operator, representing a cubic component of the crystalline electric field, $F = 180B_4^0 - 36B_4^4$ is the fourth-order spin operator, representing a component of the crystalline electric field that is axially symmetric with respect to the $\vec{c}$ -axis, $B_k^q$ are the extended Stevens operators of the electron spin, $A_{\parallel}$ and $A_{\perp}$ are the components of hyperfine interaction tensor, $Q$ is the nuclear quadrupole moment, $I$ is the nuclear spin, and $S$ is the electron spin, respectively.

A small distribution of the zero-field splitting, so-called *DStrain*, was considered during the simulations of the EPR spectra of $Mn^{2+}$ ions.

The spin-lattice relaxation time ($T_1$) was determined by fitting the echo inversion-recovery amplitude with a biexponential function:

$$I_{echo}(t) = I_1\exp\left(-t/T_1\right) + I_{SD}\exp\left(-t/T_{SD}\right), \quad (2)$$

where $I_1$ and $I_{SD}$ are the amplitudes, and $T_{SD}$ is the spectral diffusion time that affects the inversion recovery pulse sequence. Therefore, only the slower component $T_1$ was considered.

The phase memory time ($T_M$) values were obtained from the ESE decay traces fitted by a stretched exponential function:

$$I(t) = I(0)\exp\left(-t/T_M\right), \quad (3)$$

where $I(t)$ is the ESE intensity at the time $t$.

## 3. Results and discussion

In the temperature range from 297 to 5 K, a line sextet due to hyperfine interaction with $^{55}$Mn nuclei ($I$ = 5/2, 100% abundance) along with a broad line were observed in the CW EPR spectra. The broad line changes its magnetic resonance position and width upon the temperature decrease and rotation of magnetic field along the $\vec{c}$-axis, whereas the $Mn^{2+}$ spectrum position remains unchanged.

Fig. 1 shows the temperature dependence of the CW EPR spectra of the $Zn_{1-x}Mn_xSe:Fe^{2+},Cr^{2+}$ ($x$ = 0.3) crystal measured at φ = 90° ($\vec{B} \perp \vec{c}$) in the temperature range from 150 to 5 K. As can be seen from this figure, additional lines (marked with asterisks) appear in the CW EPR spectra at $T$ = 5 K.

### 3.1. $Mn^{2+}$ centers

It follows from Fig. 1 that the intensity of the sextet caused by hyperfine interaction with $^{55}$Mn decreases, and the spectra distort when the temperature decreases. This effect may be explained by extension of spin relaxation times of this paramagnetic center. In such case, two-pulse FS ESE spectra can be measured to overcome the spectral distortion.

The first derivative of the two-pulsed FS ESE spectra of the $Zn_{1-x}Mn_xSe:Fe^{2+},Cr^{2+}$ ($x$ = 0.3) crystals measured at $T$ = 5 K is presented in Fig. 2. The experimental spectrum was fitted by Eq. (1) with the following parameters: $g_{\|} = g_{\perp} = 2.0060(3)$, $A_{\|} = A_{\perp} = 61.84 \cdot 10^{-4}$ cm$^{-1}$, $D = -7.1 \cdot 10^{-4}$ cm$^{-1}$, and $DStrain = 2.97 \cdot 10^{-4}$ cm$^{-1}$.

It should be noted that apart from $Mn^{2+}$, no other paramagnetic centers presented in Fig. 1 showed an ESE signal due to their short relaxation times.

Fig. 3 shows temperature dependences of $T_1^{-1}$ and $T_M^{-1}$ rates obtained from the echo inversion-recovery amplitude and ESE decay traces measured at the resonance magnetic field position of the $Mn^{2+}$ center ($B_0$ = 350.29 mT).

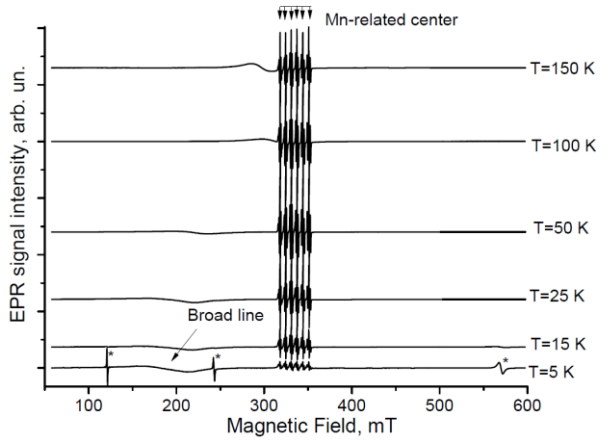


**Fig. 1.** Temperature dependence of CW EPR spectra of $Zn_{1-x}Mn_xSe:Fe^{2+},Cr^{2+}$ ($x$ = 0.3) crystals in the temperature range from 150 to 5 K. φ = 90°.

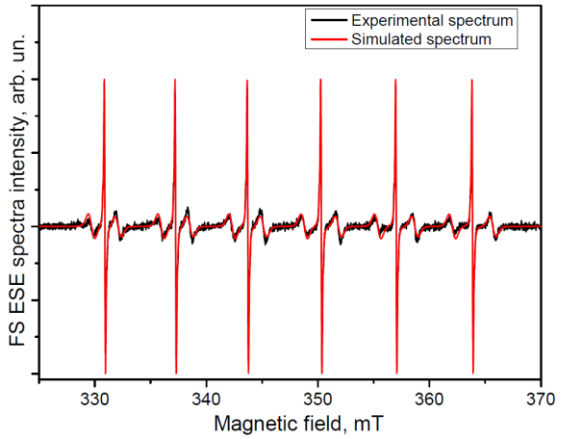


**Fig. 2.** First derivative of two-pulse FS ESE spectrum of $Mn^{2+}$ center in $Zn_{1-x}Mn_xSe:Fe^{2+},Cr^{2+}$ ($x$ = 0.3) crystal measured at φ = 0° and $T$ = 5 K. Black solid line is the experimental spectrum, red solid line is the result of fitting the experimental spectrum by Eq. (1). (Color online)

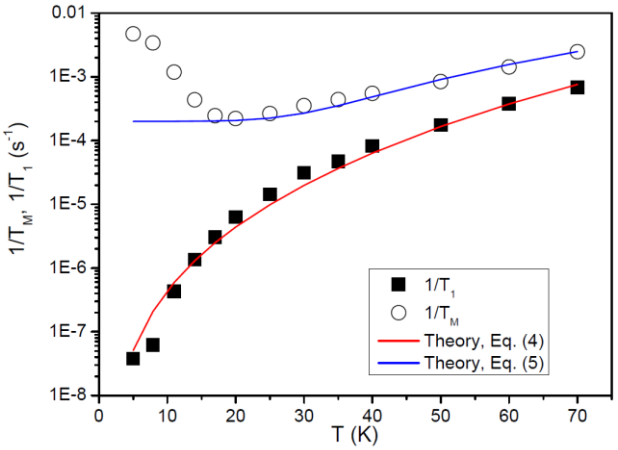


**Fig. 3.** Temperature dependence of $T_1^{-1}$ (solid squares) and $T_M^{-1}$ (open circles) for $Mn^{2+}$ center in $Zn_{1-x}Mn_xSe:Fe^{2+},Cr^{2+}$ ($x$ = 0.3) crystals. Dots are the experimental data obtained by Eqs. (2) and (3). Solid lines are the results of fitting by Eqs. (4) and (5).

The temperature dependence of $T_1^{-1}$ for $Mn^{2+}$ center shown in Fig. 3 was described taking into account the vibration modes localized at a structural defect [16], and was fitted by a linear combination of the following terms (Raman processes):

$$T_1^{-1}(T) = c_1 T^3 + c_2 T^5, \quad (4)$$

where $c_1$ and $c_2$ are the coefficients depending on the characteristics of the relaxation mechanism.

Fitting the experimental data presented in Fig. 3 by Eq. (6), the values $c_1 = 4 \cdot 10^{-10}$ K$^{-3}$·s$^{-1}$ and $c_2 = 3.7 \cdot 10^{-13}$ K$^{-5}$·s$^{-1}$ were found.

Temperature dependence of the dephasing rate $T_M^{-1}$ for $Mn^{2+}$ center can be written as follows:

$$T_M^{-1}(T) = T_{M,0}^{-1} + T_1^{-1}(T) + c\exp(-\Delta/kT), \quad (5)$$

where $T_{M,0}^{-1}$ is the temperature-independent contribution from spectral diffusion, and the third term is due to the

contribution from libration motion through the energy barrier Δ or/and from excitations to the energy level higher by Δ value.

Fitting the experimental data shown in Fig. 3 by Eq. (5) provides the following parameter values: $T_{M,0}^{-1}$ = $2\cdot10^{-4}$ $s^{-1}$, Δ = 15.5 meV = 179.8 K, and $c = 2\cdot10^{-2}$ $s^{-1}$.

According to [17], a slight increase in decoherence below 15 K may be defined by a significant contribution of instantaneous and spectral diffusion.

### 3.2. $Cr^{2+}$ centers

Fig. 4a shows angular dependence of the EPR spectra of the $Zn_{1-x}Mn_xSe:Fe^{2+},Cr^{2+}$ ($x$ = 0.3) crystals measured at $T$ = 5 K in the magnetic field being rotated from φ = 0° ($\vec{B} \parallel \vec{c}$) to φ = 180° (the rotation axis is [111]).

The red solid line in Fig. 4a shows the results of fitting the EPR spectra of $Cr^{2+}$ ion in ZnSe using the literature data presented in [9] and Eq. (1) with the following spin Hamiltonian parameters: $g_\perp$ = 1.98, $g_\parallel$ = 1.961, $D$ = –2.48 $cm^{-1}$, and $a$ = 0.02 $cm^{-1}$. Therefore,

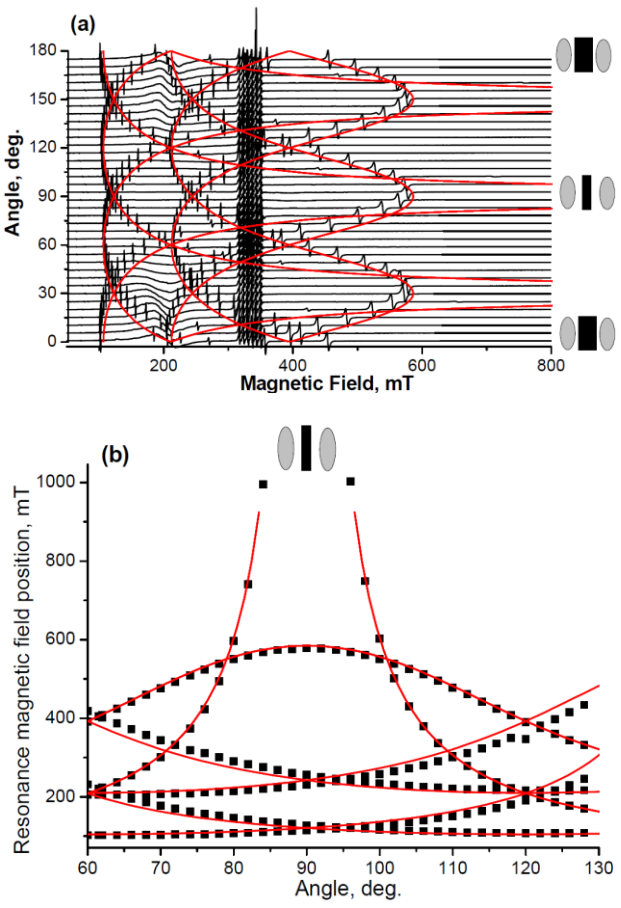


**Fig. 4.** Angular dependence of CW EPR spectra of $Zn_{1-x}Mn_xSe:Fe^{2+},Cr^{2+}$ ($x$ = 0.3) crystals measured at φ = 0° to φ = 180° (a) and detailed analysis of the angular dependence of the resonance magnetic field position of $Cr^{2+}$ ions (solid circles) at φ = 90°. $T$ = 5 K (b). Red solid lines are the result of fitting spin Hamiltonian parameters for $Cr^{2+}$ ions using Eq. (1) and the data from [9].

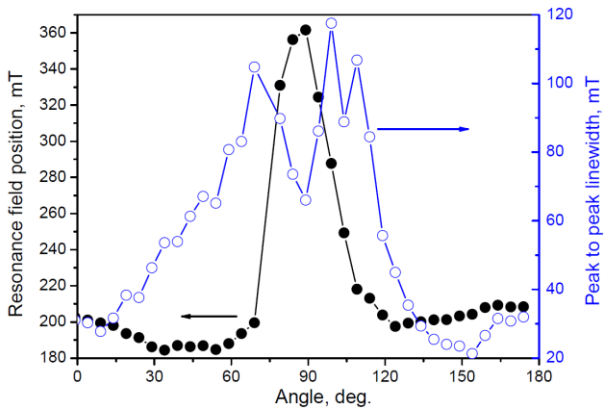


**Fig. 5.** Angular dependence of resonance field position (solid black circles) and linewidth (open blue circles) for the FMR line observed in the CW EPR spectra of $Zn_{1-x}Mn_xSe:Fe^{2+},Cr^{2+}$ ($x$ = 0.3) crystals at $T$ = 5 K. The solid lines are guides to eye.

the lines appearing in the CW EPR spectrum at 5 K should be related to the $Cr^{2+}$ ions in ZnSe.

Fig. 4b shows a detailed analysis of the angular dependence of the resonance magnetic field position of the EPR lines measured at 5 K around φ = 90°, which supports the conclusion above.

### 3.3. FMR line

The angular dependence of broad line in Fig. 1 that changes with temperature was studied in detail. Angular dependence of the resonance field position and the linewidth of this broad line was obtained at $T$ = 5 K rotating the magnetic field from φ = 0° to φ = 180° (see Fig. 5). We may conclude from the character of the obtained dependences shown in Fig. 5 that the observed broad line should be related to ferromagnetic resonance (FMR).

The behavior of anisotropy of FMR line similar to that for magnetic thin films was previously observed for a Co-implanted $BaTiO_3$ perovskite crystal [18]. This phenomenon may be ascribed to dipole-dipole interaction between magnetic nanoparticles generated by high-fluence implantation. As the distances between these particles approach their sizes, the dipole-dipole interaction couples the particle magnetic moments. Hence, a granular phase exhibits ferromagnetic continuum behavior with respect to the dipole-dipole interactions even in the absence of direct particle-to-particle contact [18]. Since we deal with high concentrations of $Cr^{2+}$ and $Fe^{2+}$ ions in our samples, we may also relate the anisotropic behavior of the FMR signal to the formation of a granular magnetic layer in the $Zn_{1-x}Mn_xSe:Fe^{2+},Cr^{2+}$ ($x$ = 0.3) crystals.

On the other hand, the latest study of $Zn_{1-x}Mn_xSe:Fe^{2+},Cr^{2+}$ ($x$ = 0.3) crystals predicts formation of $Cr^{2+}$–$Fe^{2+}$ clusters, which results in a change in the spectral properties of both $Cr^{2+}$ and $Fr^{2+}$ ions due to the modification of the local environment [19]. Therefore, appearance of the FMR signal due to the formation of $Cr^{2+}$–$Fe^{2+}$ clusters cannot be excluded as well.

The fact that no EPR signals from isolated $Fe^{2+}$ ions were observed supports the assumptions above. However, a detailed magnetization and structural study of $Zn_{1-x}Mn_xSe:Fe^{2+},Cr^{2+}$ ($x = 0.3$) crystals is required to confirm them.

## 4. Conclusions

We have studied the $Zn_{1-x}Mn_xSe:Fe^{2+},Cr^{2+}$ ($x = 0.3$) crystals with concentrations of $Cr^{2+}$ and $Fe^{2+}$ active ions of about $3\cdot10^{18}$ and $5\cdot10^{18}$ $cm^{-3}$, respectively, synthesized by the high-pressure Bridgman method. Three types of centers were observed in the EPR spectra. The first one is the sextet formed by $Mn^{2+}$ ions with $g_{||} = g_{\perp} = 2.0060(3)$, $A_{||} = A_{\perp} = 61.84\cdot10^{-4}$ $cm^{-1}$, and $D = -7.1\cdot10^{-4}$ $cm^{-1}$. Temperature dependence of the spin-lattice relaxation rate for the $Mn^{2+}$ center was described by a linear combination of two Raman processes, $\sim T^3$ and $\sim T^5$, whereas the temperature dependence of the phase memory rate was described using the Orbach process concept with $\Delta = 15.5$ meV. The second-type paramagnetic center was related to $Cr^{2+}$ ions with $g_{\perp} = 1.98$, $g_{||} = 1.961$, $D = -2.48$ $cm^{-1}$, and $a = 0.02$ $cm^{-1}$. The third broad anisotropic line was related to the appearance of FMR. Further magnetization and structural study of $Zn_{1-x}Mn_xSe:Fe^{2+},Cr^{2+}$ ($x = 0.3$) crystals is required to reveal the nature of FMR signal.

**Acknowledgments**

The authors are grateful to Dr. N. Kovalenko (Helmut Schmidt University, Hamburg, Germany) for supplying samples for the study.

**References**

1. Singh N.B., Su C., Arnold B. *et al*. Morphological and optical characteristics of transition metal doped PVT grown zinc selenide single crystal. *Cryst. Res. Technol*. 2019. **54**, No 4. P. 1800231 (10 p.). https://doi.org/10.1002/crat.201800231.
2. DeLoach L.D., Page R.H., Wilke G.D. *et al*. Transition metal-doped zinc chalcogenides: spectroscopy and laser demonstration of a new class of gain media. *IEEE J. Quantum Electron.* 1996. **32**, No 6. P. 885–895. https://doi.org/10.1109/3.502365.
3. Jelínek M., Doroshenko M.E., Jelínková H. *et al*. $Zn_{1-x}Mn_xSe:Fe^{2+},Cr^{2+}$ (x = 0.3) laser operation in a region 4.4 – 4.65 μm at 78 K pumped by a 1.94 μm Tm fiber laser through $Cr^{2+} \rightarrow Fe^{2+}$ energy transfer. *Laser Congress 2019* (ASSL, LAC, LS&C), OSA Tech. Dig. (Optica Publ. Group, 2019), P. ATu4A.5. https://doi.org/10.1364/ASSL.2019.ATu4A.5.
4. Říha A., Jelínková H., Doroshenko M.E. *et al*. Mid-IR lasing of $Fe^{2+}$ ions *via* $Cr^{2+} \rightarrow Fe^{2+}$ energy transfer process with YLF:Er or laser diode pumping at 1.7 μm. *Opt. Mater. Express*. 2020. **10**, No 2. P. 662–673. https://doi.org/10.1364/OME.384392.
5. Doroshenko M.E., Jelínková H., Osiko V.V. *et al*. Fe:ZnMnSe laser active material at 1300–1307 K: Spectroscopic properties and laser generation at 4.2–5.0 μm. *J. Lumin.* 2017. **192**. P. 1300–1307. https://doi.org/10.1016/j.jlumin.2017.09.014.
6. Doroshenko M., Jelínková H., Říha A. *et al*. Mid-IR (4.4 μm) $Zn_{1-x}Mn_xSe:Cr^{2+},Fe^{2+}$ (x = 0.3) laser pumped by 1.7 μm laser using $Cr^{2+}$-$Fe^{2+}$ energy transfer. *Opt. Lett.* 2019. **44**, No 11. P. 2724–2727. https://doi.org/10.1364/OL.44.002724.
7. Doroshenko M.E., Jelínek M., Říha A. *et al*. Long-pulse 4.4–4.6 μm laser oscillations of $Fe^{2+}$ ions in a $Zn_{1-x}Mn_xSe$ (x = 0.3) crystal pumped by a 1940 nm Tm:fiber laser through $Cr^{2+} \rightarrow Fe^{2+}$ energy transfer. *Opt. Lett.* 2019. **44**, No 21. P. 5334–5337. https://doi.org/10.1364/OL.44.005334.
8. Kreissl J., Gehlhoff W. EPR investigations of ZnS:Mn and ZnSe:Mn single crystals, powders, thin-film structures. *phys. status solidi (a)*. 1984. **81**, No 2. P. 701–707. https://doi.org/10.1002/pssa.2210810234.
9. Vallin J.T. and Watkins G.D. EPR of $Cr^{2+}$ in II-VI lattices. *Phys. Rev. B*. 1974. **9**, No 5. P. 2051–2072. https://doi.org/10.1103/PhysRevB.9.2051.
10. Kramushchenko D.D., Ilyin I.V., Soltamova V.A. *et al*. EPR diagnostics of laser materials based on ZnSe crystals doped with transition elements. *Phys. Solid State*. 2013. **55**, No. 2. P. 269–277. https://doi.org/10.1134/S1063783413020169.
11. Kramushchenko D.D., Asatryan H.R., Khramtsov V.A. *et al*. EPR method for investigation and diagnosis materials promising for quantum electronics ($PbGa_2S_4$, ZnSe). *J. Phys. Conf. Ser*. 2013. **461**. P. 012031 (7 p.). https://doi.org/10.1088/1742-6596/461/1/012031.
12. Surma M., Godlewski M. Efficient two-center Auger mechanism of electron trapping by $Fe^{3+}$ ions in ZnSe: Fe, Cr. *Acta Phys. Pol. A*. 1997. **92**, No. 5. P. 1017–1020. https://doi.org/10.12693/APhysPolA.92.1017.
13. Vazhenin V.A., Potapov A.P., Shakurov G.S. *et al*. Paramagnetic defects in ZnSe crystals doped with iron ions. *Phys. Solid State*. 2017. **59**, No 10. P. 1993–2001. https://doi.org/10.1134/S106378341710033X.
14. Říha A., Jelínková H., Doroshenko M.E. *et al*. Mid-infrared laser generation of $Zn_{1-x}Mn_xSe$ and $Zn_{1-x}Mg_xSe$ (x≈0.3) single crystals co-doped by $Cr^{2+}$ and $Fe^{2+}$ ions – Comparison of different excitation wavelengths. *Materials*. 2022. **15**. P. 5277 (15 p.). https://doi.org/10.3390/ma15155277.
15. Stoll S., Schweiger A. EasySpin, a comprehensive software package for spectral simulation and analysis in EPR. *J. Magn. Reson*. 2006. **178**, No 1. P. 42–55. https://doi.org/10.1016/j.jmr.2005.08.013.
16. Vichery H., Rullier-Albenque F., Bouffard S. E.P.R. study of electron irradiation defects in the red molybdenum bronze of potassium $K_{0.33}MoO_3$. *J. Phys. France*. 1989. **50**, No 6. P. 685–696. https://doi.org/10.1051/jphys:01989005006068500.
17. Mentink-Vigier F., Binet L., Gourier D. Vezin H. Origin of the decoherence of the extended electron spin state in Ti-doped β-$Ga_2O_3$. *J. Phys.: Condens. Matter*. 2013. **25**. P. 316002 (8 p.). https://doi.org/10.1088/0953-8984/25/31/316002.

18. Kazan S., Mikailzade F.A., Şale A.G. *et al*. Magnetic properties of Co-implanted $BaTiO_3$ perovskite crystal. *Phys. Rev. B*. 2010. **82**, No 5. P. 054402 (10 p.). https://doi.org/10.1103/PhysRevB.82.054402.
19. Doroshenko M.E., Jelinkova H. $Cr^{2+}$–$Fe^{2+}$ clusters formation in $Zn_{1-x}Mn_xSe$ crystal. *Opt. Spectrosc.* 2023. **131**, No 4. P. 429–434. https://doi.org/10.61011/EOS.2023.04.56351.72-22.

**Authors and CV**

**Dariya V. Savchenko**, Doctor of Sciences in Physics and Mathematics, Acting Head of the Department of General Physics and Modelling of Physical Processes of the National Technical University of Ukraine "Igor Sikorsky Kyiv Polytechnic Institute" and Senior Researcher at the Technical center NAS of Ukraine. The area of her scientific interests includes magnetic resonance in semiconductors, dielectrics and biomaterials.
https://orcid.org/0000-0002-0005-0732

**Bekir E. Bekirov**, PhD, Researcher at the Radiospectroscopy Department, O. Usikov Institute for Radiophysics and Electronics, NAS of Ukraine. The area of his scientific interests includes radiospectroscopy of diluted semiconductors.
E-mail: bekirbekirov1986@gmail.com

**Igor V. Ivanchenko**, Doctor of Sciences in Radiophysics, Leading Researcher at the Radiospectroscopy Department, O. Usikov Institute for Radiophysics and Electronics, NAS of Ukraine. The area of his scientific interests includes radiospectroscopy of diluted semiconductors.
E-mail: ivanchenkoi534@gmail.com,
https://orcid.org/0000-0003-2540-4995

**Nina A. Popenko**, Doctor of Sciences in Radiophysics, Leading Researcher at the Radiospectroscopy Department, O. Usikov Institute for Radiophysics and Electronics, NAS of Ukraine. The area of her scientific interests includes radiospectroscopy of diluted semiconductors.
E-mail: ireburan@yahoo.com

**Ekaterina N. Kalabukhova,** Doctor of Sciences in Physics and Mathematics, Leading Researcher at the Department of Semiconductor Heterostructures, V. Lashkaryov Institute of Semiconductor Physics, NAS of Ukraine. The area of her scientific interests includes magnetic resonance in semiconductor and nanosized materials.
E-mail: kalabukhova@yahoo.com,
https://orcid.org/0000-0003-0272-9471

**Authors' contributions**

**Savchenko D.V.:** methodology, investigation, software, formal analysis, data curation, writing – original draft, writing – review & editing.
**Ivanchenko I.V.:** conceptualization, writing – review & editing.
**Popenko N.A.:** methodology, validation, writing – review & editing.
**Bekirov B.E.:** formal analysis, data curation (partially), writing – original draft, visualization.
**Kalabukhova E.N.:** supervision, writing – review& editing.

**Електронні та магнітні властивості монокристалів $Zn_{1-x}Mn_xSe:Fe^{2+},Cr^{2+}$ (x = 0.3)**

**Д.В. Савченко, І.В. Іванченко, Н.А. Попенко, Б.Е. Бекіров, К.М. Калабухова**

**Анотація.** Методами стаціонарної та імпульсної спектроскопії електронного парамагнітного резонансу (ЕПР) вперше досліджено кристали $Zn_{1-x}Mn_xSe:Fe^{2+},Cr^{2+}$ ($x$ = 0.3). Використання переваг імпульсного ЕПР дозволило отримати параметри спінового Гамільтоніана для іонів $Mn^{2+}$ ($g_{||} = g_{\perp} = 2.0060(3)$, $A_{||} = A_{\perp} = 61.84\cdot10^{-4}$ см$^{-1}$, $D = -7.1\cdot10^{-4}$ см$^{-1}$). Температурну залежність часів спінової релаксації для іонів $Mn^{2+}$ було описано за допомогою процесу Орбаха для $T_M^{-1}$ та механізмів Рамана для $T_1^{-1}$. З аналізу кутової залежності спектрів стаціонарного ЕПР було визначено параметри спінового Гамільтоніана для іонів $Cr^{2+}$ ($g_{\perp} = 1.98$, $g_{||} = 1.961$, $D = -2.48$ см$^{-1}$, $a = 0.02$ см$^{-1}$). Додатково спостерігали лінію, що відповідає анізотропному феромагнітному резонансу, природа якої ще має бути з'ясована.

**Ключові слова:** ЕПР, перехідні метали, селенід цинку.